Eutopic Endometrium From Women With Endometriosis Shows Altered Ultrastructure and Glycosylation Compared to That From Healthy Controls—A Pilot Observational Study

Carolyn J. P. Jones, PhD, **Ibrahim M. Inuwa, PhD**, **Luciano G. Nardo, MD**, **Pietro Litta, MD**, and **Asgerally T. Fazleabas, PhD**

Maternal and Fetal Health Research Centre, School of Clinical and Laboratory Science, University of Manchester, Manchester, United Kingdom (CJPJ, LGN); Department of Human and Clinical Anatomy, Sultan Qaboos University Hospital, Sultanate of Oman (IMI); Department of Reproductive Medicine, St Mary's Hospital, Manchester, United Kingdom (LGN); Department of Obstetrics and Gynaecology, University of Padua, Italy (PL); and Department of Obstetrics and Gynecology, University of Illinois at Chicago, Chicago, Illinois (ATF).

Abstract

Endometrial curettings from a cohort of 24 women with endometriosis were compared with matched biopsies from 14 healthy, fertile women and examined for ultrastructural changes and the secretion of glycans bound by the lectin from *Dolichos biflorus*. Ultrastructural analysis of glandular endometrial tissue from women with stages I to III endometriosis showed heterogeneous responses to the disease, biopsies often showing a mixture of features, combining delays in the maturation sequence with characteristics of later phenotypes particularly in the mid-late secretory phase of the menstrual cycle. Expression of glycans bound by *Dolichos biflorus* agglutinin was very variable in these cases but generally matched the observed ultrastructure. Biopsies from women with stage IV endometriosis showed immature gland morphology later in the cycle and also failed to express *Dolichos biflorus* agglutinin–binding glycans, suggesting an association between histological and biochemical function in advanced disease states. These findings may explain in part endometriosis-associated subfertility as blastocyst attachment is intimately associated with appropriate glycosylation and gland morphology.

Keywords

Endometriosis; endometrium; glycosylation; ultrastructure; human

INTRODUCTION

Endometriosis is defined as the extrauterine growth of endometrial glandular epithelial and stromal cells, generally found over pelvic peritoneal and visceral surfaces. It affects about 10% of women in the reproductive age group,[1] increasing to 30% in patients with infertility and up to 45% in patients with chronic pelvic pain,[2] and is one of the most common causes

Address correspondence to: Carolyn J. P. Jones, PhD, Research Floor, Maternal and Fetal Health Research Group, University of Manchester, St Mary's Hospital, Hathersage Road, Manchester M13 0JH, United Kingdom. carolyn.jones@manchester.ac.uk.

of infertility and chronic pelvic pain. Although existence of this disease has been known for over a century, our current knowledge of its pathogenesis, the pathophysiology of related infertility, and its spontaneous appearance is limited.

Experimental models of endometriosis have been developed in rodents[3,4] and in the nonhuman primate[5,6] to overcome the ethical and practical issues limiting research in humans. Studies using a baboon model have elegantly demonstrated that intrapelvic injection of endometrial curetting caused pelvic endometriosis and decreased pregnancy rates.[7,8] The baboon model has also been used to investigate the aberrant expression of several genes in endometrial tissue.[9–11]

More recently, we have used the primate model of induced endometriosis to examine the ultrastructure of eutopic and ectopic endometrium by light and electron microscopy as well as the expression of glycans by lectin histochemistry. The results indicated that endometriotic tissue is characterized by significant changes both in the gland architecture and in glycosylation compared to normal endometrium,[12] with the premature appearance of features normally associated with late stages of the cycle. Nevertheless, there remains a lack of knowledge of the ultrastructural and biochemical changes in endometrial tissues in humans.

In the current pilot study, we extend our observations to biopsies obtained from a carefully selected group of women with visually and histologically proven endometriosis and controls without the disease, examining both the ultrastructure of the glandular tissue and the expression of glycans bound by *Dolichos biflorus* agglutinin[13] (DBA). In this way, we hope to assess whether accelerated maturation of gland architecture and biochemistry, which was described in the baboon model, is also a feature in the human. Indeed, the examination of this type of epithelial glycosylation offers a sensitive and unique assessment of normal tissue cycling and changes occasioned by pathology. It is hoped that inspection of tissue from this cohort of women may give some insight into the etiology of endometriosis by means of establishing whether there are any indications of the derivations of the various lesions.

MATERIALS AND METHODS

Study Population

A total of 38 women of reproductive age with regular menstrual cycles (28–32 days) and without any history of autoimmune disease were recruited. Of these participants, we had 24 women (study group, mean age 34, range 22–45 years) with visually and biopsy-proven endo-metriosis who had undergone endometrial curettage and laparoscopic excision of endometriotic deposits and 14 fertile women (control group, mean age 34, range 25–44 years) without endometriosis who had undergone endometrial curettage only for the purpose of the study. The demographic details of the 2 groups were comparable (data not shown). All women with endometriosis complained of pelvic pain, deep dyspareunia, and/or sub-fertility. None of the participants had an intrauterine device in situ or had received hormonal therapy in the 3 months preceding laparoscopy and endometrial sampling. Endometriosis at the time of laparoscopy was staged according to the revised American Fertility Society (rAFS) scoring system[14] and confirmation of dating of control specimens was undertaken by one of

us (I.M.I.) using stereological techniques on ultrathin sections (see below). As no significant ultrastructural abnormalities were apparent in 4 endometriotic biopsies taken between days 2 and 9, only those cases from day 13 onward will be described in detail.

The study was approved by the Local Research Ethics Committee (Ref No 06/Q1407/173) as well as by the Universities of Manchester, United Kingdom, and Padua, Italy. All women gave written informed consent to participate in the study.

Tissue

Tissue was received from 2 sites: Department of Obstetrics and Gynaecology, University of Padua, Italy (from P. Litta, specimens coded PL), and Department of Reproductive Medicine, Central Manchester and Manchester Children's University Hospitals NHS Trust, Manchester, United Kingdom (from L. G. Nardo, specimens coded NE). All chemicals and reagents were obtained from Sigma (UK or Italy) unless otherwise specified. Tissue from Padua was fixed in half-strength Karnovsky fixative (2% w/v parafor-maldehyde and 2.5% glutaraldehyde [v/v] in 0.1 M phosphate buffer pH 7.2) for 24 to 48 hours, then rinsed in buffer and transported to the United Kingdom. The material from Manchester was either fixed in half-strength Karnovsky fixative (as above) if available or in neutral buffered formalin and then refixed in 2.5% glutaraldehyde in 0.1 M sodium cacodylate buffer pH 7.2 (Agar Scientific Ltd, Stansted, UK) for 2 to 3 hours when received in the laboratory. Both sets of tissue were diced into 1-mm thick slices before further processing and divided into 2 parts. One part was postfixed in 1% osmium tetroxide (Agar Scientific Ltd)/1.5% potassium ferrocyanide in 0.05 M sodium cacodylate buffer pH 7.2 for 1 hour in the dark, rinsed twice in buffer, dehydrated, and processed into Taab epoxy resin (TAAB Laboratories Equipment Ltd, Aldermaston, UK) for electron microscopy. The other part was not osmicated but otherwise processed in the same way for lectin histochemistry. Semithin 0.5-μm sections were cut on a Reichert Ultracut microtome using a diamond knife, stained with 1% toluidine blue in 1% borax on a hotplate, and suitable areas containing glands and/or surface epithelium selected for further examination.

Electron Microscopy

Ultrathin sections of the osmicated material, 70-nm thick, were mounted on 200 mesh copper grids and contrasted with uranyl acetate (Agar Scientific Ltd)/lead citrate and examined in a Philips CM10. Digital images of optimally orientated glandular epithelium were captured using a Deben camera and stored as 4-MB TIFF files.

Endometrial Morphometry

Digital TEM images acquired were loaded onto *Histometrix*, a stereology software (Histometrix MIL6, Kinetic Imaging Ltd, UK) installed on an IBM compatible personal computer. The software was used to estimate the parameters below.

Nuclear volume density ($V_{f(nuc)}$)—The volume density, V_f, of nucleus in cytoplasm of surface epithelia was estimated by point counting.[15,16] Briefly, this was obtained by generating a grid with an array of random points on the image and counting the total number of points, P falling within the nucleus (P_{nuc}) and dividing it by the number of points

falling within the whole cell (P_{cell}). The volume fraction of nucleus in the cell, $V_{\text{f(nuc)}}$, is given by

$$V_{\text{f(nuc)}} = \frac{\sum P_{\text{nuc}}}{\sum P_{\text{cell}}}.$$

Absolute volume of nucleus of surface epithelial cell ($\bar{V}_{\text{nuc}}$)—Surface epithelial cell nucleus volume was determined by point-sampled intercept method.[17] On 4 randomly selected images showing whole cells from each sample, an unbiased counting frame with superimposed random test points was applied. If a test point falls on a nucleus profile, a line, l_0, in an isotropic uniform direction (IUR) was drawn through the point to the nuclear boundary. The volume of the nucleus, $\bar{V}_{\text{nuc}}$, was then estimated from the following equation:

$$\bar{V}_{\text{nuc}} = \frac{\pi}{3} \times \sum l_0^3.$$

Absolute surface epithelial cell volume (V_{cell})—Estimates of surface epithelial volume, V_{cell}, was obtained using the volume density of the nucleus and nuclear volume (see above):

$$V_{\text{cell}} = \frac{\bar{V}_{\text{nuc}}}{V_{\text{f(nuc)}}}.$$

Lectin Histochemistry

Sections 0.75-μm thick were cut and mounted on 3-aminopropyltriethoxysilane-coated slides,[18] dried in an oven at 50°C for 2 days, and then stained with biotinylated *Dolichos biflorus* lectin as previously described.[12] Epoxy resin was removed with saturated sodium ethoxide diluted 1:1 with absolute ethanol, followed by washes in ethanol and distilled water, then endogenous peroxidase was blocked with 10% (v/v) hydrogen peroxide (BDH, Poole, UK) before exposure to 0.03% trypsin (w/v; type II-S) in 0.05 M Tris-buffered saline (TBS) pH 7.6 for 4 minutes at 37° C. After washing, sections were incubated with 10 μg/mL biotinylated lectin from *Dolichos biflorus* in 0.05 MTBS containing 1-mmol/L calcium chloride for 1 hour at 37°C, washed in the same buffer, then treated with 5 μg/mL avidin peroxidase in 0.125 M TBS, pH 7.6, with 0.347 M sodium chloride for 1 hour at 37°C.[19] Sections were washed and sites of lectin binding revealed with 0.05% (w/v) diaminobenzidine tetrahydrochloride dihydrate in 0.05 M TBS, pH 7.6, and 0.015% (v/v) hydrogen peroxide (100 volumes) for 5 minutes at 18 ± 0.5°C. Sections were rinsed, airdried, and mounted in neutral synthetic mounting medium (BDH).

Negative controls were carried out by substitution of 0.05 M TBS pH 7.6 with added calcium for the lectin to identify any nonspecific binding of avidin peroxidase to the tissue section or the presence of residual endogenous peroxidase activity. Sections were also incubated with the lectin in the presence of 0.2 M *N*-acetyl galactosamine to block binding

of the lectin. Sections were assessed using a semiquantitative ranking system of analysis, where staining intensity was allocated a grade from – (negative) to ++++ (intense staining).

RESULTS

Control Specimens (Nonendometriotic)

The ultrastructure of normal glandular epithelium has been fully described in the literature[20–24] and so only a brief summary, restricted to main features, of the changes observed from day 9 onward through the menstrual cycle will be described here (Figure 1) and in Table 1.

Mid-late proliferative—At 9 days, nuclei were basally situated and euchromatic with a smooth outline; several mitoses were visible (*, Figure 1A). Small or elongated mitochondria and vertically orientated Golgi with narrow saccules and inconspicuous cisternae of endoplasmic reticulum were seen; lateral membranes were generally straight. Small aggregates of glycogen were beginning to form basally (G, Figure 1A). Some secretory droplets and heterophagosomes[21] were present. By day 14, there was generally more subnuclear glycogen though mitoses were still evident in 1 specimen.

Early secretory—Basal deposits of glycogen were seen in day 17 specimens (Gly, Figure 1B), which had polarized cells, long parallel supranuclear cisternae of endoplasmic reticulum, and Golgi saccules. Some nuclei contained nucleolar channel systems (Figure 1C) typical of days 17 to 20, whereas giant mitochondria were sometimes present basally (Figure 1D). Desmosomes were well developed on lateral membranes, which were more tortuous.

Mid-secretory to late secretory—Large cytoplasmic projections (pinopods) generally devoid of organelles and characteristic of days 19 to 22 were seen (Figure 1E). By day 24, many of the nuclei were heterochromatic and glycogen was scattered throughout the cell (Figure 1F). Mitochondria were mainly basal and lateral membranes convoluted. Some Golgi saccules and secretory droplets but few endoplasmic reticulum cisternae were present. Later, cells became more cuboidal with basal nuclei and glycogen foci more scattered. Subnuclear fat droplets were present and there was increased lateral membrane interdigitations (arrow, Figure 1G); by day 27, occasional large heteroly-sosomes were also present (Figure 1H).

Eutopic Endometriotic Endometrium

Proliferative phase (days 2–13)—The proliferative phase eutopic endometrium from women with endometriosis (day 2 [stage II], day 5 [stage III], day 7 [stage I], and day 9 [stage II]) did not show any significant differences from that obtained from healthy controls. Mitotic figures were found (*, Figure 2A) and some cells had small clumps of glycogen within. No secretions were observed. At day 9, there was some evidence of heterophagosome formation (Figure 2B) as in controls; by day 13, in a stage IV specimen (PL6), mitotic figures were still present but there was some heterogeneity in the nuclear morphology (Table 2).

Early secretory phase (days 15–18)—The specimen from day 16 (PL8, stage I-II) was probably from the late proliferative phase (Figure 2C) with euchromatic, basal nuclei and mitotic figures. There were numerous apical secretory droplets, with scant glycogen production and no evidence of nucleolar channel formation. The 2 day 15 specimens were very different from each other, yet both showed later than expected phenotypes. One (PL1, stage I) had a very heterogeneous morphology, some glands exhibiting characteristics of a mid-secretory phenotype, with occasional pinopods normally seen on days 19 to 20 and glandular cells rich in dispersed glycogen (Figure 2D); other glands were more like controls with heavy basal deposits of glycogen. There were also dilated glands with cuboidal cells, suggestive of a later phenotype and heavy luminal secretions. Complex nucleoli showed some evidence of nucleolar channel systems. The other 15-day specimen (PL17, stage III), with only a few glands, had a much later phenotype with little intracellular glycogen, heterochromatic nuclei, and complex lateral membrane interdigitations (Figure 2E).

The 3 day 17 specimens were variable in their morphology. Several mitotic figures were seen in 1 (PL21, Figure 2F), despite the presence of masses of glycogen, suggesting asynchrony in differentiation though this specimen was only at stage I of the disease process. Some glands showed a more appropriate ultrastructure, with numerous Golgi stacks and cisternae of rough endoplasmic reticulum. PL5 (stage III) also had large aggregates of glycogen in some glands (Figure 2G), and both had some enlarged mitochondria though no fully formed nucleolar channel systems were seen. In PL5, there were some cuboidal epithelial cells in dilated glands with clusters of mitochondria, though nuclei were large and euchromatic and there was little evidence of protein biosynthesis (Figure 2H). The third day 17 case (PL27, stage III) also showed a mixture of features with narrow glands of columnar cells with oval, euchromatic nuclei, similar to those seen in the proliferative phase (Figure 2I). However, there were also late secretory features: dispersed glycogen, basal fat droplets, and lateral membrane interdigitations with intercellular spaces basally. Intraepithelial leucocytes were present with some heterophagosomes.

The day 18 specimen showed occasional nucleolar channel systems and enlarged (though not "giant") mitochondria. Even though this was at stage IV of the disease, mitotic figures were not seen and the appearance was consistent with that expected for the time in the menstrual cycle.

Mid-secretory phase (days 19–24)—A day 19 specimen (PL12, stage II) showed delayed maturation (Figure 3A) with glands of columnar cells with little glycogen and an absence of both nucleolar channel systems and giant mitochondria, while a day 20 specimen (PL23, stage III) contained both these features typical of days 17 to 20 (Figure 3B). Columnar cells had aggregates of glycogen basally and sometimes apically though often also finely dispersed.

Of 3 day 21 specimens examined, 1 (PL28, stage II) showed features of a late secretory phenotype with dilated glands of cuboidal cells, though nuclei were round, euchromatic, and basally situated (Figure 3C), and there were only occasional aggregates of glycogen. Many supra-nuclear mitochondria and small apical vacuoles with amorphous contents were present with fat droplets basally. Lateral membranes were straight with few interdigitations, and

there were some intercellular spaces. The other 2 specimens (PL36, stage I and PL31, stage III) were more typical for their dates, cells being columnar and with more heterochromatic nuclei, vertically orientated Golgi bodies, and occasional aggregates of glycogen (G, Figure 3D). Cells containing large secondary lysosomes were seen in PL36 but no fat droplets were evident in either case.

The day 22 (stage II) and one of the day 24 specimens (PL25, stage IV) showed features of a much earlier phenotype, with mitotic figures (Figure 3E) and abundant glycogen in subnuclear and supranuclear locations. Some nuclei were more irregular with condensed peripheral chromatin; in the day 22 biopsy, these were generally associated with dilated glands and cuboidal cells with small round mitochondria such as is found later in the cycle. Lateral membranes showed well-developed interdigitations basally. The cells of the second day 24 biopsy (PL26, stage III) were more typical of the mid-secretory phase, being columnar with heterochromatic nuclei and finely dispersed glycogen (Figure 3F). In dilated glands, the cells were more cuboidal, with irregular apical plasma membranes and scant microvilli.

Late secretory phase (days 25–29)—Mixed features were found in one of the day 25 specimens (PL30, stage III) with very regular, basal, euchromatic nuclei in columnar cells with dispersed aggregates of glycogen and clusters of fat droplets (F, Figure 3G). The other (PL33, also stage III) contained more heterochromatic nuclei, though a minority were euchromatic and more regular. A nucleolar channel system was seen in 1 cell, while fat droplets typical of the late secretory phase were found in others (Figure 3H). Some glands contained scattered glycogen rosettes, while others had none. Intercellular spaces were often present in both cases with loose interdigitations between the cells (Figure 3H).

The day 27 specimen (stage IV) was rather anomalous, with glands of rather low, cuboidal cells, euchromatic nuclei, and sparse organelles—mitochondria were not clustered basally as expected—nor were lateral membranes showing interdigitation as is usually found at that stage in the cycle (Figure 4A).

The day 29 specimen (PL29, stage III) also showed mixed features with widely dilated glands of columnar rather than cuboidal cells and variable nuclear morphology. Glycogen was more aggregated than expected (Figure 4B). Apical vacuoles with diffuse contents, sometimes with a dense core, were present (Figure 4C), and large intracellular inclusions with heterogeneous contents were frequently seen (Figure 4D). Basal fat droplets and an irregular basal plasma membrane was present, though lateral membrane interdigitations were not prominent (Figure 4B).

Lectin Histochemistry

Control endometrium—Binding of the lectin from *Dolichos biflorus* (DBA) to *N*-acetyl galactosamine-containing sequences, including GalNAcα1,3(LFucα1,2)Galβ1,3/4-GlcNAcβ1—is not generally found in the proliferative phase endometrial glands (Figure 5A) but occurs during the mid-secretory to late secretory phase of the menstrual cycle (Figure 5B). Occasional foci of stain can be seen on some cell apices as early as day 9, possibly because of adhesion of previously secreted products to cell surfaces. There was a general

increase in binding during the course of the secretory phase, with stained glands often alternating with unstained (see Table 1).

Endometriotic endometrium—Specimens from women with stages I to III endometriosis showed extremely variable staining with DBA, with levels of staining generally associated with the late secretory phase sometimes appearing much earlier in the cycle (eg, day 17) and weak staining when more binding would normally be expected. Biopsies from women with grade IV endometriosis, however, completely failed to express any DBA-binding glycans and apart from 1 day 13 specimen (PL6), which was not expected to show staining, was invariably associated with a gland pattern suggestive of an earlier phase of the cycle, with narrow tubular glands composed of an epithelium with basally situated nuclei (Figure 5C and E; see Table 2).

DISCUSSION

In this pilot study, we have demonstrated that eutopic endometrium from women with endometriosis may have significant biochemical and ultrastructural differences from normal control tissue and these changes appear to become marked particularly in the mid-secretory part of the cycle. One of the most striking and important abnormalities was the complete absence of DBA-binding glycans in endometrium from women with stage IV endometriosis, and in 2 of the 3 cases from the midsecretory to late secretory phase, this was in keeping with morphological evidence of a proliferative phase phenotype and delay in maturation. More specimens with stage IV endometriosis are, of course, required to confirm these initial findings. The specimen from day 24 (PL25) of the cycle had mitotic figures at the ultrastructural level; none were seen in the day 27 endometrium (PL22), but some glands contained nuclei that were round and euchromatic, suggestive of a newly divided state, and the ultrastructure of the cells was unusual for that stage in the cycle. Women with stages I to III generally showed DBA binding appropriate or even increased for the time in the cycle, apart from a case with stage II disease, which had negligible binding on day 22 of the cycle associated with the presence of mitotic figures. These morphological changes in women with endometriosis are in agreement with the alterations in gene expression patterns that have been recently reported.[25] These studies demonstrated that in women with moderate-to-severe disease, there is an abnormal transition from the proliferative to early secretory phase, which is associated with the inability of progesterone to downregulate DNA synthesis and cellular proliferation. Thus, our results provide a morphological correlation with the molecular evidence for the attenuation of the action of progesterone in the eutopic endometrium of women with endometriosis.

It is thus plausible to speculate that such results at stage IV disease are indicative of progesterone resistance. This has been reported in endometriosis[26] together with deficiency in 17-β-hydroxysteroid dehydrogenase type 2 in glandular epithelial cells.[27] Aromatase activity, which catalyses the conversion of C_{19} steroids to estrogens, has also been found to be elevated in eutopic endometrium from women with endometriosis[28] and has been thought to be a factor that sustains the endometriotic lesions, partially or totally mediated by estrogen receptor a-positive stromal cells[29] present in lesions.[30] Kao and colleagues[31] found dysregulation of glycodelin, which is under the regulation of progesterone, in women with

endometriosis and suggested that this, too, is consistent with progesterone resistance and proposed that its underexpression may contribute to the reported low implantation rates and reduced fertility. It is interesting to observe, however, that despite abnormalities in the distribution of steroid receptors and concomitant changes in both structure and function of uterine glands, menstruation and cycle length appear to be unaffected. The absence of changes in cycle length in both baboons[32] and women with endometriosis may reflect the ability of progesterone to prevent the endometrium from regression because of the presence of a sufficient number of progesterone receptors for basal action but an insufficient responsiveness to progesterone to induce appropriate morphological transformation or gene expression during the secretory phase.[33,34]

Previous studies on the endometrium in women with and without endometriosis have suffered from the lack of objectivity and well-fixed material, hence making the interpretation of data difficult and controversial. We were fortunate in obtaining well-preserved eutopic endometrial tissue that has enabled fine detail of the cells to be examined. The influence of the cycle length and the dysfunction of the hypothalamus-pituitary-ovary axis were not an issue as the main inclusion criteria for the study were regular cycles and no hormonal therapy for a period of at least 3 months before sampling. Although it was not possible to test the women for the LH (luteinizing hormone) surge, morphometry was used to confirm the dating of samples as well as ultrastructural markers such as the presence of the nucleolar channel system and giant mitochondria, which helped to offset the variation in gland ultrastructure seen in the secretory phase. Nuclear morphology was found to be very variable, and some control and endometriotic specimens showed very euchromatic nuclei in the mid to late secretory phase, which was a surprising finding as most reports of endometrial ultrastructure describe heterochromatic nuclei in the late secretory phase.[20–22]

Eutopic endometrium from women with endometriosis did not show any specific ultrastructural abnormalities compared to that from normal women, and in the proliferative phase, there were no significant differences in the ultrastructural features of the 2 tissues. Later in the cycle, however, features normally confined to particular stages appeared over a much wider period of time. Hence, mitotic figures—not usually seen beyond days 14 to 16 of the cycle—were observed in 3 cases on days 17, 22, and 24, those cells in the process of cell division on days 17 and 24 being associated with intracellular glycogen, a feature never seen in control cases where cell division is normally segregated chronologically from glycogen biosynthesis. Likewise, giant mitochondria were observed later than in the controls. Euchromatic nuclei were a consistent finding throughout the secretory phase but, unlike the controls, were not always accompanied by areas of glands with heterochromatic nuclei later in the cycle, and glycogen deposits also tended to be more prominent later in the cycle compared to controls, which started to show diminished amounts after day 17. Other specimens had phenotypes more characteristic of midsecretory to late secretory phase. Sometimes nuclei were heterochromatic, as in a day 19 specimen but often they were euchromatic, a feature seen sometimes in controls but more generally associated with the proliferative phase. As can be seen from Table 2, there was also considerable variation between specimens obtained on the same day of the cycle, for instance, on days 15, 17, and 24, with respect to the incidence of mitoses and deposition of glycogen.

The presence of late mitoses is consistent with the recent findings of Burney and colleagues[25] who observed the maintenance of a proliferative molecular profile in the early secretory endometrium from women with endome-triosis, with an enrichment of genes involved in cell cycle regulation. They concluded that the pathways governing the transition from the proliferative to differentiated state were dysfunctional in the women with endometriosis. They suggested that nonsteroidal signaling pathways may also be involved. Dysregulation of cell cycle genes such as *GOS2* and *SALP* (Sam68-like phosphotyrosine protein a) has also been described in endometrium from women with endometriosis[31] and this, too, may contribute toward alteration in mitotic activity. The presence of dividing cells well into the secretory phase is also consistent with findings of decreased apoptosis in eutopic endometrium from women with endometriosis compared to healthy controls,[35] indicating abnormal survival of eutopic endometrial cells throughout the entire menstrual cycle. Higher expression of Ki67 was also reported in endometriotic glands in the proliferative phase and early-and mid-secretory phases,[36] while transforming growth factor (TGF)-β1 remained unchanged in these endometria, unlike normal glands that showed an increase.

In conclusion, our study has demonstrated significant differences in the biology of eutopic endometriotic and normal endometrium, both in the tissue architecture and the biochemistry. In advanced disease, the gland epithelium in the secretory part of the cycle showed a delay in maturation both morphologically and also in the expression of DBA-binding glycans. Several researchers have shown that pelvic endometriosis is heterogeneous in its clinical manifestations and response to treatment[37–39]; however, these findings may explain some of the fertility problems associated with endometriosis, as receptivity is intimately bound up with the morphology and especially glycosylation of the uterine tissues. Previous studies have shown that treatment of women with RU484 is associated with a block in the normal expression of the glycans bound by DBA[40] and, in the cases examined here, defects in steroid receptor may be eliciting the same phenomena. Further studies are therefore required to examine the distribution of these receptors in suitably fixed material.

Acknowledgments

REFERENCES

1. Eskenazi B, Warner ML. Epidemiology of endometriosis. Obstet Gynecol Clin North Am. 1997; 24:235–258. [PubMed: 9163765]

2. Gruppo Italiano Per lo Studio Dell'endometriosi. Prevalence and anatomical distribution of endometriosis in women with selected gynecological conditions: results from a multicentric Italian study. Hum Reprod. 1994; 9:1158–1162. [PubMed: 7962393]

3. Awwad JT, Sayegh RA, Tao XJ, Hassan T, Awwas ST, Isaacson K. The SCID mouse: an experimental model for endometriosis. Hum Reprod. 1999; 14:3107–3111. [PubMed: 10601104]

4. Rossi G, Somigliana E, Moschetta M, et al. Dynamic aspects of endometriosis in a mouse model through analysis of implantation and progression. Arch Gynecol Obstet. 2000; 263:102–107. [PubMed: 10763836]

5. D'Hooghe TM. Clinical relevance of the baboon as a model for the study of endometriosis. Fertil Steril. 1997; 68:613–625. [PubMed: 9341599]

6. Fazleabas AT, Brudney A, Gurates B, Chai D, Bulun S. A modified baboon model for endometriosis. Ann N Y Acad Sci USA. 2002; 55:308–317.

7. D'Hooghe TM, Bambra CS, Raeymaekers SCM, De Jonge I, Lauweryns JM, Koninckx PR. Intrapelvic injection of menstrual endometrium causes endometriosis in baboons (Papio cynocephalus and Papio anubis). Am J Obstet Gynecol. 1995; 173:125–134. [PubMed: 7631669]

8. D'Hooghe TM, Riday AM, Bambra CS, Suleman MA, Raeymaekers SCM, Koninckx PR. The cycle pregnancy rate is normal in baboons with stage I endometriosis but decreased in primates with stage II and III-IV disease. Fertil Steril. 1996; 66:809–813. [PubMed: 8893690]

9. Gashaw I, Hastings JM, Jackson K, Winterhager E, Fazleabas AT. Induced endometriosis in baboons (Papio anu-bis) increases the expression of the proangiogenic factor Cyr61 (CCN1) in the eutopic and ectopic endometria. Biol Reprod. 2006; 74:1060–1066. [PubMed: 16481591]

10. Hastings JM, Jackson KS, Mavrogianis PA, Fazleabas AT. The estrogen early response gene, FOS, is altered in a baboon model of endometriosis. Biol Reprod. 2006; 75:176–182. [PubMed: 16672717]

11. Kim JJ, Taylor HS, Lu Z, et al. Alterations in HOXA10 expression in endometriosis: potential role in decidualization. Mol Hum Reprod. 2007; 13:323–332. [PubMed: 17350963]

12. Jones CJP, Denton J, Fazleabas AT. Morphological and glyco-sylation changes associated with the endometrium and ectopic lesions in a baboon model of endometriosis. Hum Reprod. 2006; 21:3068–3080. [PubMed: 17018533]

13. Baker DA, Sugii S, Kabat EA, Ratcliffe RM, Hermentin P, Lemieux RU. Immunochemical studies on the combining sites of Forssman hapten reactive hemagglutinins from *Dolichos biflorus, Helix pomatia and Wistaria floribunda*. Biochemistry. 1983; 22:2741–2750. [PubMed: 6603233]

14. American Society for Reproductive Medicine. Revised American Society for Reproductive Medicine classification of endometriosis. Fertil Steril. 1996; 67:817–821.

15. Weibel, ER. Vol 1: Practical Methods for Biological Morphometry. London: Academic Press; 1979. Stereological Methods.

16. Reed MG, Howard CV. Surface weighted star-volume: concept and estimation. J Microsc. 1998; 190:350–356. [PubMed: 9674159]

17. Gundersen HJG, Jensen EB. Stereological estimation of the volume-weighted mean volume of arbitrary particles observed on random sections. J Microsc. 1985; 138:27–142.

18. Maddox PH, Jenkins D. 3'Aminopropyltriethoxysilane (APES): a new advance in section adhesion. J Clin Pathol. 1987; 40:1256–1260. [PubMed: 3316291]

19. Jones CJP, Mosley S, Jeffrey IJM, Stoddart RW. Elimination of the non-specific binding of avidin to tissue sections. Histo-chem J. 1987; 19:264–268.

20. Armstrong EM, More IAR, McSeveney D, Chatfield WR. Reappraisal of the ultrastructure of the human endometrial gland cell. J Obs Gyn Brit Comm. 1973; 80:446–460.

21. Gordon M. Cyclic changes in the fine structure of the epithelial cells of human endometrium. Int Rev Cytol. 1975; 42:127–172. [PubMed: 172466]

22. Cornillie FJ, Lauweryns JM, Brosens IA. Normal human endometrium—an ultrastructural survey. Gynecol Obstet Invest. 1985; 20:113–129. [PubMed: 4085915]

23. Dockery P, Li TC, Rogers AW, Cooke ID, Lenton EA. The ultrastructure of the glandular epithelium in the timed endo-metrial biopsy. Hum Reprod. 1988; 3:826–834. [PubMed: 3182973]

24. Dockery, P.; Burke, MJ. The fine structure of the mature human endometrium. In: Aplin, JD.; Fazleabas, AT.; Glasser, SR.; Guidice, LC., editors. The Endometrium. 2nd. London: Informa Healthcare; 2008. p. 46-65.

25. Burney RO, Talbi S, Hamilton AE, et al. Gene expression analysis of endometrium reveals progesterone resistance and candidate susceptibility genes in women with endometriosis. Endocrinology. 2007; 148:3814–3826. [PubMed: 17510236]

26. Attia GR, Zeitoun K, Edwards D, Johns A, Carr BR, Bulun SE. Progesterone receptor isoform A but not B is expressed in endo-metriosis. J Clin Endocrinol Metab. 2000; 85:2897–2902. [PubMed: 10946900]

27. Zeitoun KM, Takayama K, Sasano H, et al. Deficient 17β-hydroxysteroid dehydrogenase type 2 expression in endometriosis: failure to metabolize 17β-estradiol. J Clin Endocrinol Metab. 1998; 83:4474–4480. [PubMed: 9851796]

28. Hudelist G, Czerwenka K, Keckstein J, et al. Expression of aromatase and estrogen sulfotransferase in eutopic and ectopic endometrium: evidence for unbalanced estradiol production in endometriosis. Reprod Sci. 2007; 14:798–805. [PubMed: 18089598]

29. Cooke PS, Buchanan DL, Lubahn DB, Cunha GR. Mechanism of estrogen action: lessons from the estrogen receptor-α knockout mouse. Biol Reprod. 1998; 59:470–475. [PubMed: 9716542]

30. Matsuzaki S, Murakami T, Uehara S, Canis M, Sasano H, Okamura K. Expression of estrogen receptor alpha and beta in peritoneal and ovarian endometriosis. Fertil Steril. 2001; 75:1198–1205. [PubMed: 11384649]

31. Kao LC, Germeyer A, Tulac S, et al. Expression profiling of endometrium from women with endometriosis reveals candidate genes for disease-based implantation failure and infertility. Endocrinology. 2003; 144:2870–2881. [PubMed: 12810542]

32. Wang C, Mavrogianis PA, Fazleabas AT. Endometriosis is associated with progesterone-resistance in the oviduct: evidence based on the localization of oviductal glycoprotein 1 (OVGP1). Biol Reprod. 2009; 80:272–278. [PubMed: 18923157]

33. Jackson KS, Brudney A, Hastings JM, Mavrogianis PA, Kim JJ, Fazleabas AT. The altered distribution of the steroid hormone receptors and the chaperone immunophilin FKBP52 in a baboon model of endometriosis is associated with progesterone resistance during the window of uterine receptivity. Reprod Sci. 2007; 14:137–150. [PubMed: 17636225]

34. Bulun SE, Cheng YH, Yin P, et al. Progesterone resistance in endometriosis: link to failure to metabolize estradiol. Mol Cell Endocrinol. 2006; 248:94–103. [PubMed: 16406281]

35. Meresman GF, Vighi S, Buquet RA, Contreras-Ortiz O, Tesone M, Rumi LS. Apoptosis and expression of bcl-2 and bax in eutopic endometrium from women with endometrio-sis. Fertil Steril. 2000; 74:760–766. [PubMed: 11020520]

36. Johnson MC, Torres M, Alves A, et al. Augmented cell survival in eutopic endometrium from women with endometriosis: expression of c-myc, TGF-beta1 and bax genes. Reprod Biol Endocrinol. 2005; 3:45. [PubMed: 16150151]

37. Chapron C, Fauconnier A, Vieira M, et al. Anatomical distribution of deeply infiltrating endometriosis: surgical implications and proposition for a classification. Hum Reprod. 2003; 18:157–161. [PubMed: 12525459]

38. Abbott JA, Hawe J, Clayton RD, Garry R. The effects and effectiveness of laparoscopic excision of endometriosis: a prospective study with 2–5 year follow-up. Hum Reprod. 2003; 18:1922–1927. [PubMed: 12923150]

39. Heilier JF, Nackers F, Verougstraete V, Tonglet R, Lison D, Donnez J. Increased dioxin-like compounds in the serum of women with peritoneal endometriosis and deep endometrio-tic (adenomyotic) nodules. Fertil Steril. 2005; 84:305–312. [PubMed: 16084869]

40. Aplin JD, Jones CJP, McGinlay PB, Croxatto HB, Fazleabas AT. Progesterone regulates glycosylation in endometrium. Biochem Soc Trans. 1997; 25:1184–1187. [PubMed: 9449972]
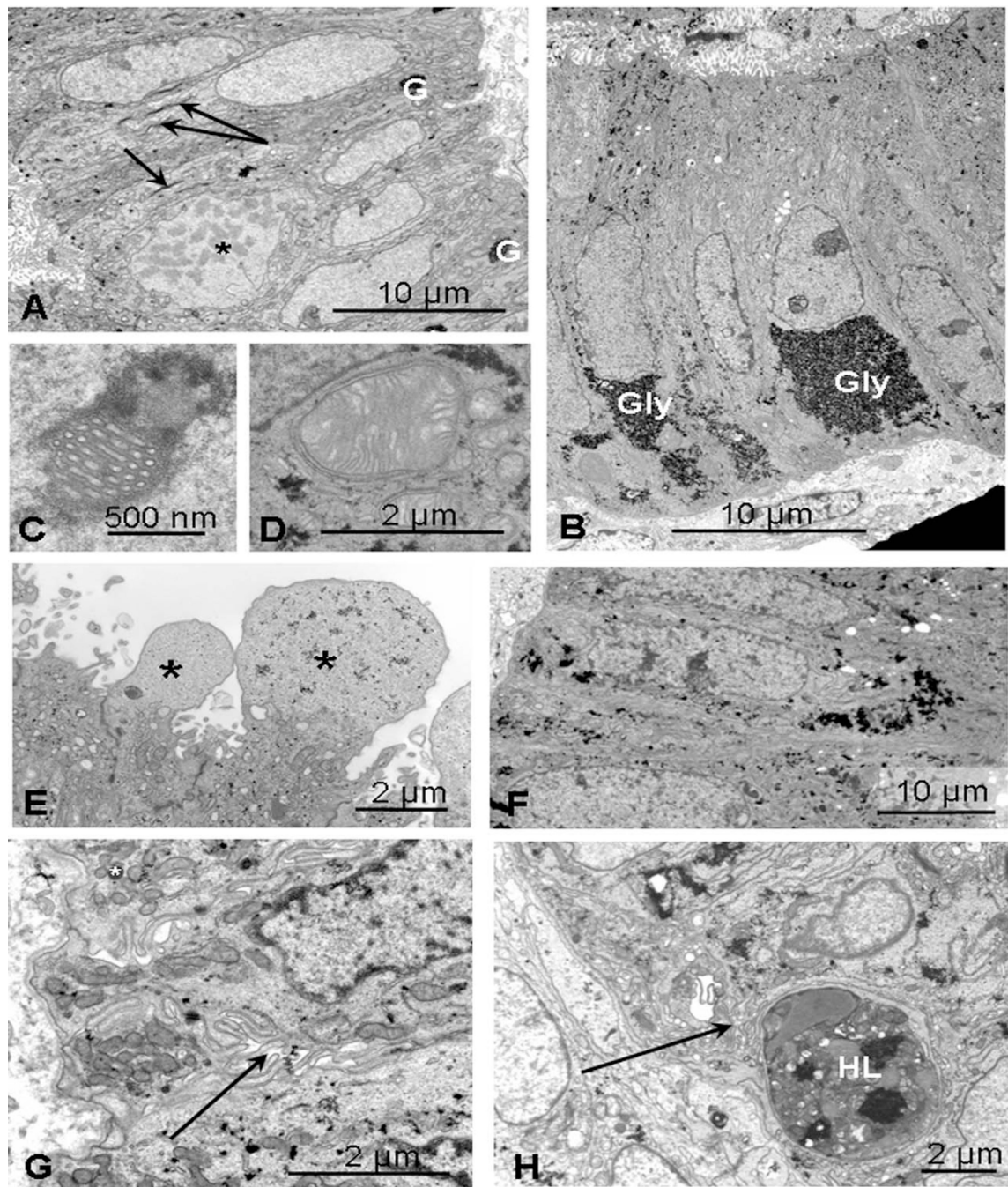
Figure 1.
Normal control endometrium. A, Mid-proliferative: day 9 specimen showing a cell undergoing mitosis (*) and smooth euchromatic nuclei, small mitochondria and vertically orientated Golgi saccules (arrows). Small basal aggregates of glycogen are visible (G). B, Early secretory: day 17 specimen with basal deposits of glycogen (Gly), supranuclear endoplasmic reticulum, and Golgi bodies. C, Nuclear channel system. D, Giant mitochondrion. E, Mid-secretory: pinopods (*) characteristic of days 19–22. F, Mid-late secretory: at day 24, diffuse, scattered aggregates of glycogen are present. G, Scattered basal

mitochondria with occasional fat droplets (*) and complex lateral interdigitations (arrow). H, Day 27 showing a large heterolysosome (HL) containing remnants of dead cells.
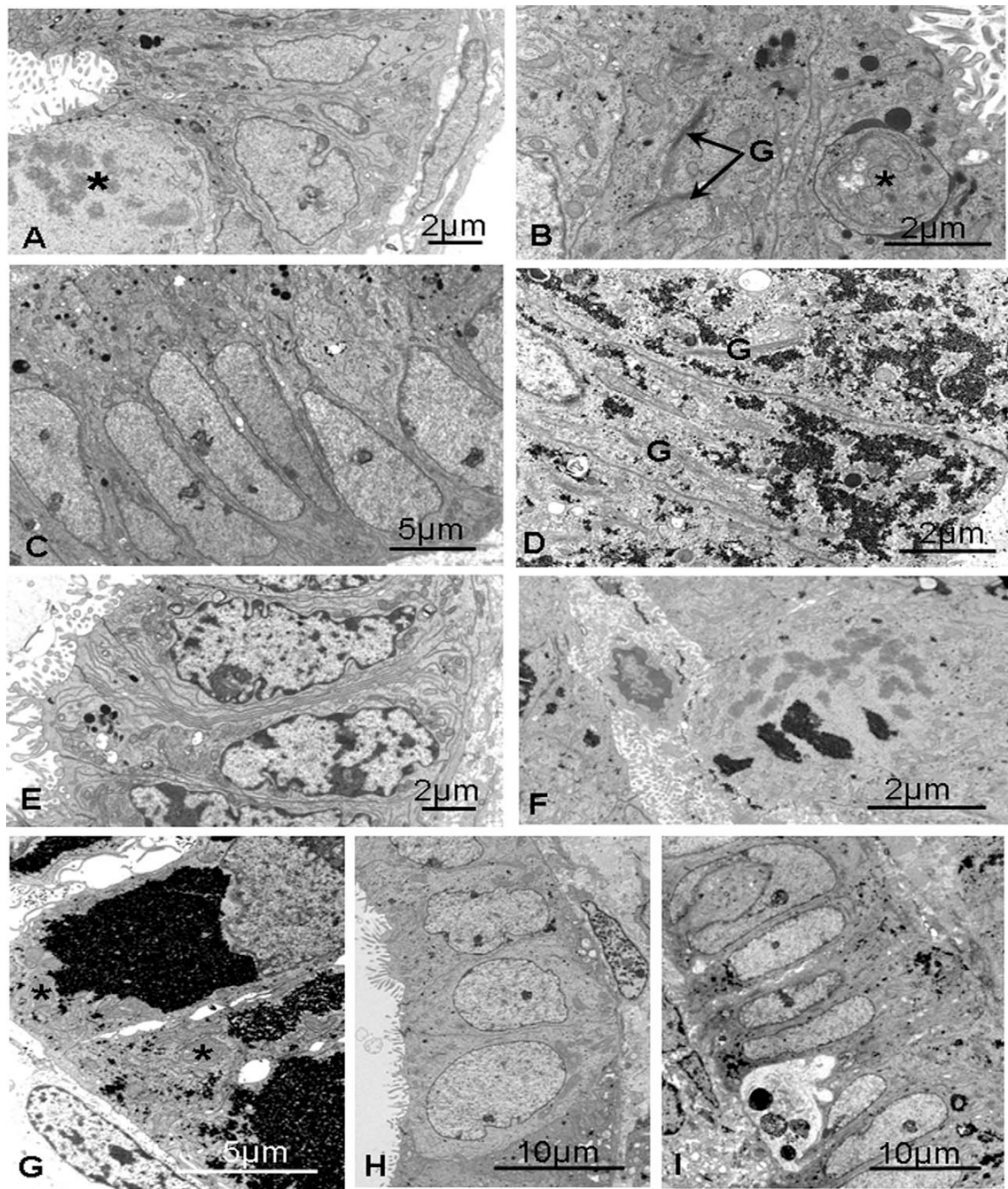
Figure 2.
Endometriotic eutopic epithelium, days 5 to 17. A, Day 5 (PL16): a mitotic figure (*) and mainly euchromatic nuclei, with fine cisternae of endoplasmic reticulum and occasional secretory droplets. B, Day 9 (PL3): secretory droplets, finely dispersed glycogen, and an early phagosome (*) with prominent Golgi saccules (G). C, Day 16 (PL8): proliferative phase–like endometrium with euchromatic nuclei and apical secretory droplets. D, Day 15 (PL1): dispersed glycogen and long, vertically orientated Golgi saccules (G). E, Day 15 (PL17): basally situated heterochromatic nuclei, small mitochondria, and complex lateral

interdigitations present a later phenotype. F, Day 17 (PL21): a cell in mitosis containing clumps of glycogen. G, Day 17 (PL5): large amounts of glycogen are present. H, Day 17 (PL5): nuclei are very euchromatic though cells are cuboidal and lacking glycogen. I, Day 17 (PL27): smooth, euchromatic nuclei together with dispersed aggregates of glycogen and an intraepithelial leucocyte with heterophagosomes.
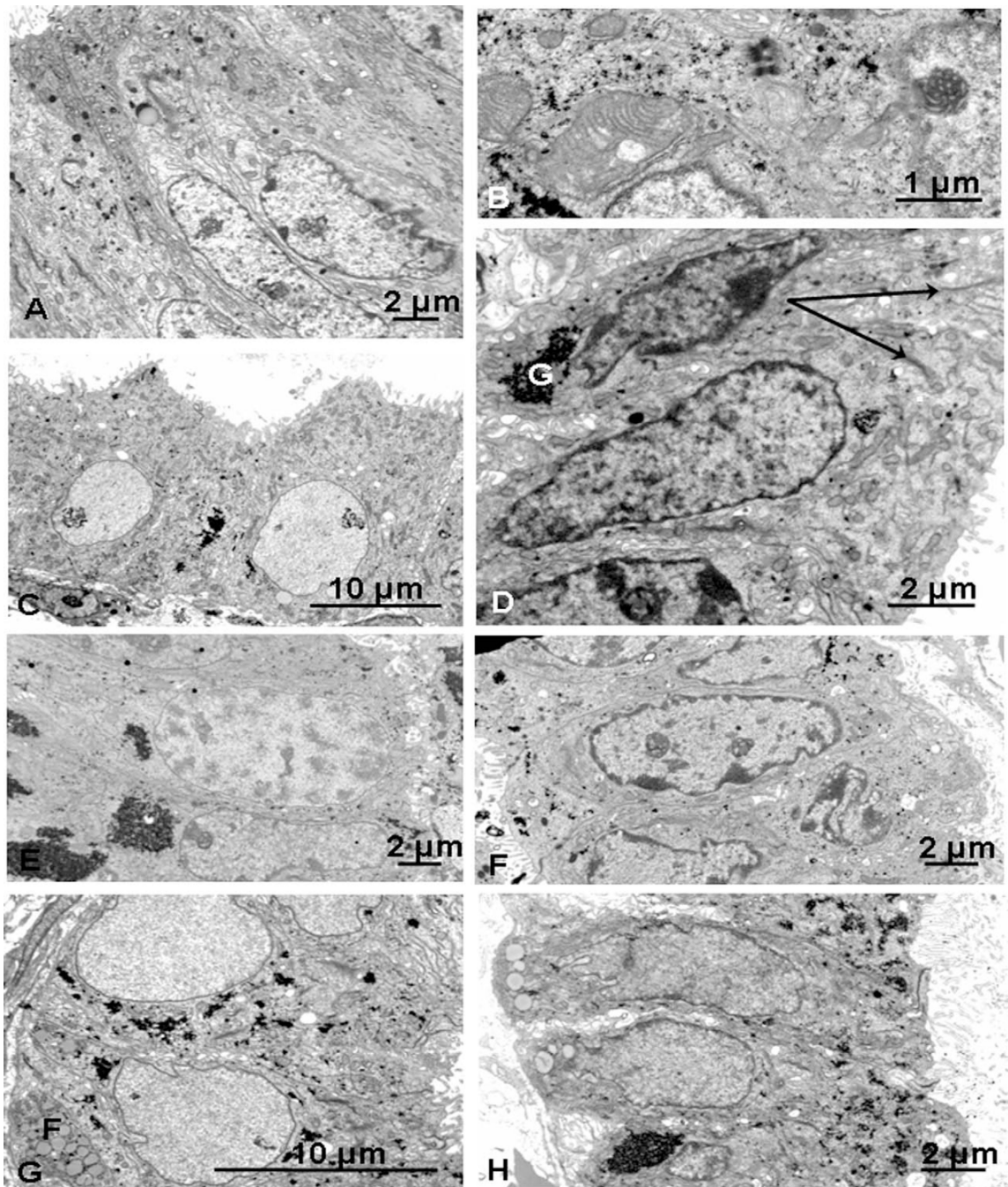
Figure 3.
Endometriotic eutopic epithelium, days 19 to 25. A, Day 19 (PL12): immature-looking cell cytoplasm with no glycogen and numerous apical secretory droplets and narrow cisternae of rough endoplasmic reticulum. B, Day 20 (PL23): giant mitochondria and a nucleolar channel system are present. C, Day 21 (PL28): dilated glands with round, basally situated euchromatic nuclei, and cytoplasm like that of the late secretory phase with occasional aggregates of glycogen. D, Day 21 (PL36): heterochromatic nuclei, occasional aggregates of glycogen (G), and short, narrow Golgi cisternae (arrows) with rod-shaped mitochondria

plentiful apically. E, Day 22 (PL20): a cell in early prophase, with cells containing large aggregates of glycogen. F, Day 24 (PL26): cells more typical of the mid-secretory phase, with heterochromatic nuclei and some scattered glycogen deposits. G, Day 25 (PL30): regular, euchromatic nuclei basally situated in cells with some glycogen and clusters of fat droplets (F) basally and Golgi saccules apically. H, Day 25 (PL33): large aggregates and scattered deposits of glycogen, and nuclei more heterochromatic than in PL030 with basal fat droplets and intercellular spaces.
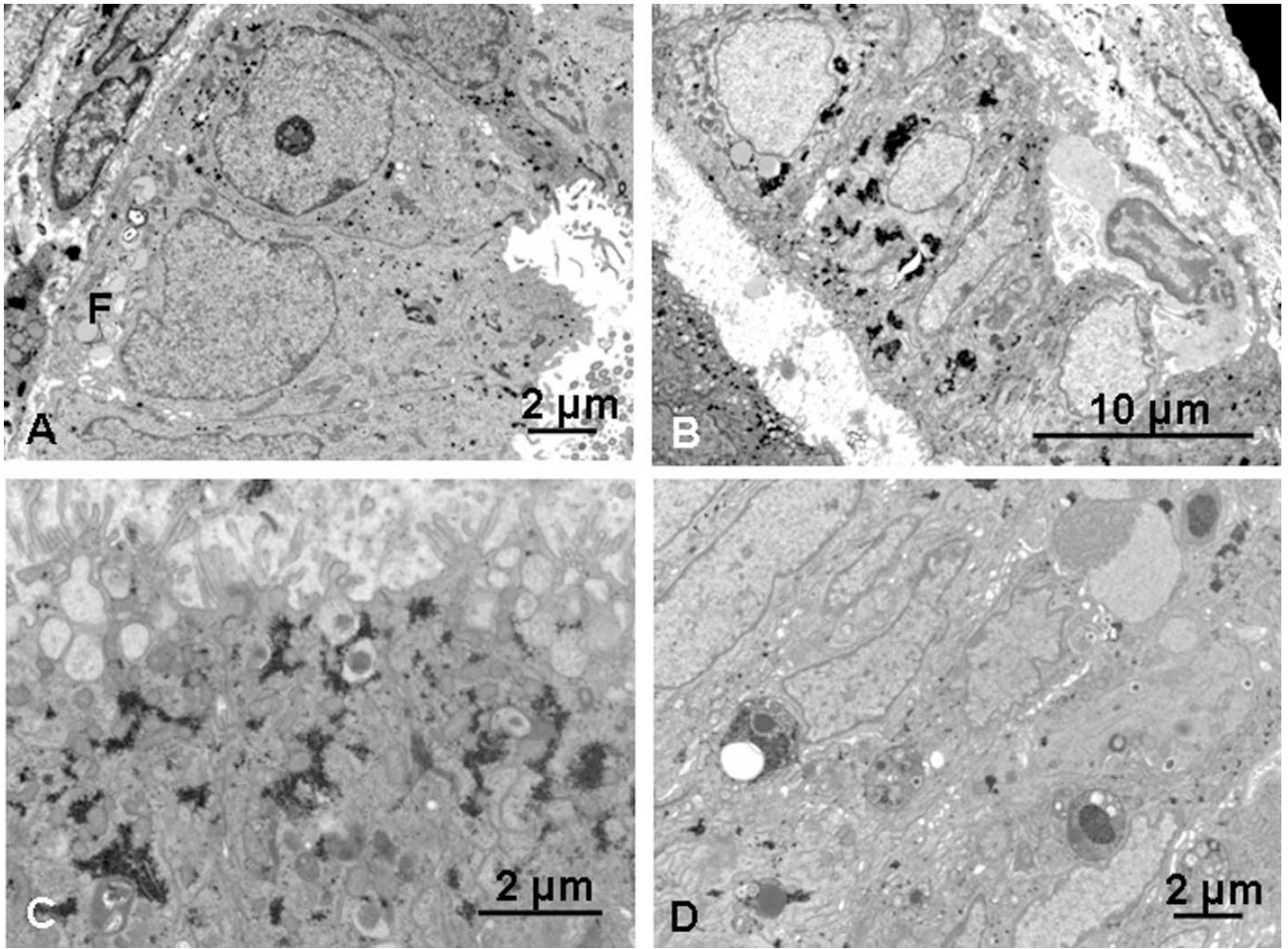
Figure 4.
Endometriotic endometrium, days 27 to 29. A, Day 27 (PL22): basally situated, euchromatic nuclei with a few fat droplets (F) basally. A few scattered remnants of glycogen and secretory droplets are present in apical cytoplasm, and microvilli are blunt. B, Day 29 (PL29): euchromatic nuclei and glycogen deposits together with occasional fat droplets, and an intraepithelial lymphocyte. C, Day 29 (PL29): apical secretory vacuoles with flocculent contents, sometimes with a dense core, are present, with some glycogen. D, Day 29 (PL29): several heterophagosomes are present, with heterogeneous contents.
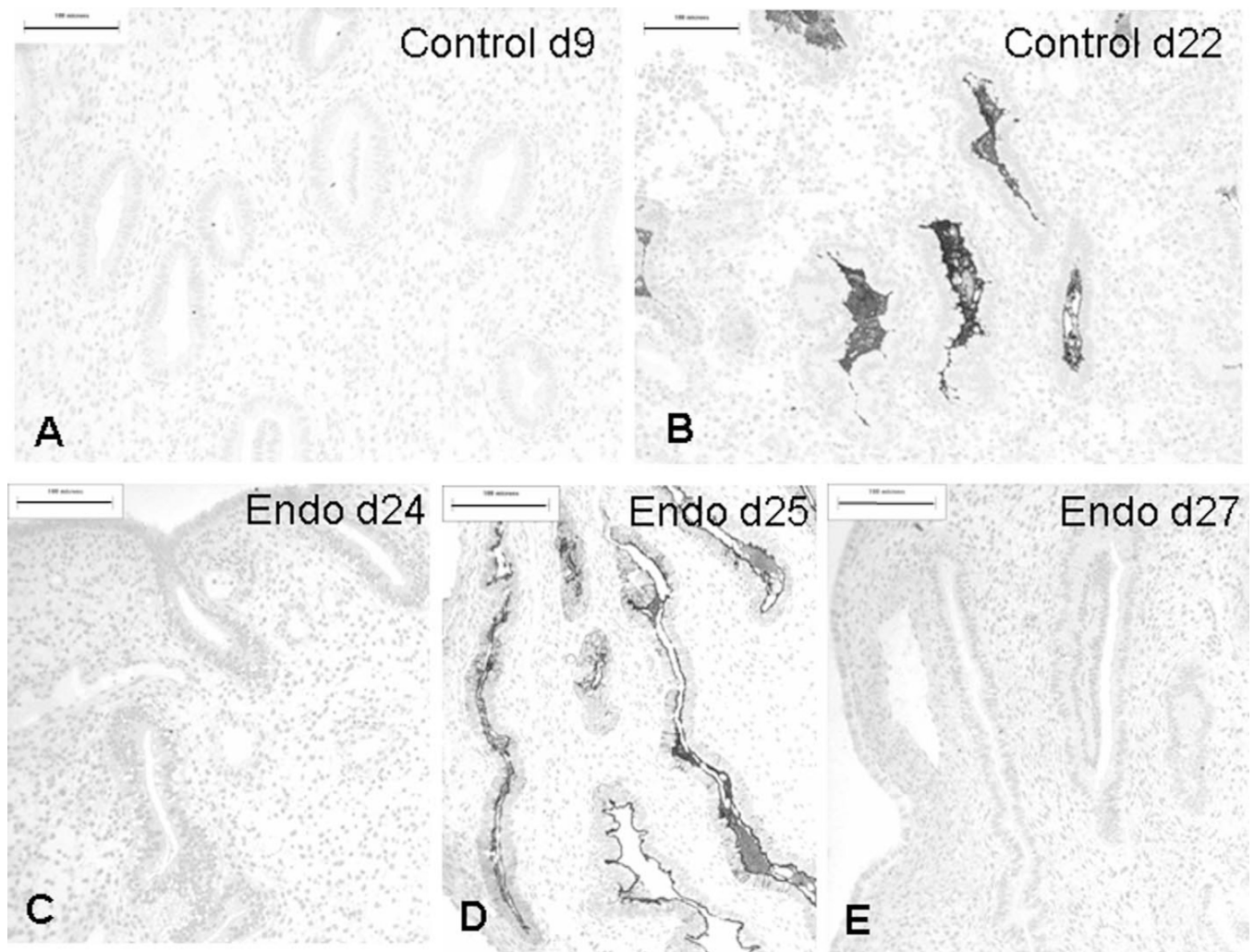
Figure 5.

Dolichos biflorus agglutinin (DBA) binding in control and endometriotic endometrium. A, Day 9 control specimen shows no binding of DBA. B, By 22 days, control endometrium shows binding of DBA to secretions in the dilated glands. C, Day 24 (PL25) endometriotic endometrium contains tubular glands with no binding of DBA. D, Day 25 (PL30) endometriotic endometrium with abundant DBA-binding glandular secretions. E, Day 27 (PL22) endometriotic endometrium with narrow, tubular glands, and complete absence of DBA binding. Scale bar: 100 μm.

Table 1

Main Features of Normal Endometrium During the Menstrual Cycle (DBA Staining From − [Absent] to +++ [Strong])

Spec No	NE9	NE2	NE4	PL13	NE8	NE1	PL18	PL7	NE10	PL35	PL2	NE11	PL4	NE12
Day of cycle	9	9	14	14	14	16	17	17	20	20	22	22	24	27
DBA staining	−/+	−/+	−	+	−	+	−	++	++	+	+++	+++	++	+++
Mitoses	+	+	+	−	−	+	−	−	−	−	−	−	−	−
Giant mitochondria	−	−	−	−	−/+	−	−	+	+	−	−/+	−	−	−
NCS	−	−	−	−	−	−	+	+	+	−	−	−	−	−
Euchromatic nuclei	+	+	+	−	+	+	−	+	+	−	−	+	−	+
Heterochromatic nuclei	−	−	−	+	−	−	+	−	+	+	+	+	−	+
Long mitochondria	−	+	−	−	+	+	+	+	+	+	−	−	+	−
Glycogen	−/+	−/+	+	+	+	−/+	++	++	++	+	+	+	+	+
Secretory droplets	++	+	+	++	++	+	+	++	+	+	+	−/+	+	+
Golgi	++	+	+	+	+	+	++	+	+	+	+	+	+	+
Lateral Interdigitations	−/+	−	−	−	+	−	?+	++	−/+	++	+	++	+	++
Fat droplets	−	−	−	−	−	−	−	−	−	−	−	+	−	−
Macrophages	−	−	−	−	+	−	−	+	−	−	−	+	−	+
Other features	Heterolys					Heterolys					Pinop	Cytoplasmic filaments		Heterolys

Abbreviations: DBA, *Dolichos biflorus* agglutinin; heterolys, heterolysosmes; NCS, nucleolar channel systems; NE, Specimens from Manchester (Nardo Endometria); pinop, pinopods; PL, specimens from Italy (P. Litta); ? = possible presence.

Table 2

Main Features of Eutopic Secretory Phase Endometrium in Women With Endometriosis (DBA Staining From – [Absent] to ++++ [Intense])

PL Spec No	6	17	1	8	5	27	21	32	12	23	28	36	31	20	25	26	30	33	22	29
Day of cycle	13	15	15	16	17	17	17	18	19	20	21	21	21	22	24	24	25	25	27	29
Stage	IV	III	I	I-II	III	III	I	IV	II	III	II	I	III	II	IV	III	III	III	IV	III
DBA stain	–	+	++	–/+	–/+	++++	++	–	+++	++	+++	++	+++	–/+	–	++++	++++	+++	–	++++
Mitoses	+	–	–	+	–	–	++/glyc	–	–	–	–	–	–	+	++/gly	–	–	–	–	–
Giant mitos	–	–	–	–	(+)	–	(+)	(+)	–	–	–	–	–	+	(+)	+	–	–	–	–
NCS	–	–	–	–	?	–	–	+	–	+	–	–	–	?	–	–	–	+	–	–
Euch nuc	+	–	+	+	+	+	+	–	+	+	+	–	+	+	+	+ (occ)	+	+	+	+
Het nuc	–	+	+	–	–	–	–	+	+	–	+	+	+	–	–	+	–	+	–	+
Long mitos	–	–	+	–	+	+	+	+	–	+	–	–	+	+	+	–	–	–	–	–
Glycogen	+	–	+++	–/+	+++	+++	+++	+++	–/+	++	+	+	+	+++	+++	+	++	++	–/+	+
Interdig	–	++	–/+	–	–	–/+	–	–/+	–	+	–/+	+	+	–	++	–/+	+	++	–/+	+
Heterolys	–	–	–	–/+	–	++	–	–	+	–	+	+	–	–	–	–	–	–	–/+	++
Pat droplets	–	–	–	–	–	+	–	–	–	–	+	–	–	–	–	–	+	+	–	+
Pinopods	–	–	+	–	–	–	–	–	–	–	–	–	–	–	–	–	–	–	–	–

Abbreviations: DBA, *Dolichos biflorus* agglutinin; euch, euchromatic nuclei; het, heterochromatic nuclei; Glyc, glycogen in mitotic figure; heterolys, heterolysosmes; interdig, interdigitation; mitos, mitochondria; (), partially formed; NCS, nucleolar channel system; PL, specimens from Italy (P. Litta).